Numerical Investigation of Effects of Ramification Length and Angle on Pressure Drop and Heat Transfer in a Ramified Microchannel

F. Kaya

Dept. of Mechanical Engineering, Nigde University, Nigde, 51240, Turkey

Email:fkaya@nigde.edu.tr

ABSTRACT

The aim of this study is to investigate the effects of ramification length and angle on pressure drop and heat transfer in a ramified microchannel. The governing equations for the fluid flow were solved by using Fluent CFD code. Computational results were compared with mathematical model values given in the literature for validation. On the basis of a water-cooled (only water and water+ethanol) smooth microchannel, ramified plates were designed into the heat sink, and then the corresponding laminar flow and heat transfer were investigated numerically. Four different configurations of ramified plates were considered by adjusting the angle and length of the T profile. Results obtained from the numerical tests show good agreement with the mathematical model and these results also demonstrate that the pressure drop increases with increasing both the ramification length and angle. Moreover, the maximum temperature inside the ramified microchannel increases with increasing the ramification length as well as increasing the ratio volume fraction of ethanol.

Keywords: Microchannel; CFD; Pressure drop; Heat transfer; Ramification length and angle.

NOMENCLATURE

c_p	heat transfer coefficient		*Subscript*	
h	specific heat		max	maximum
k	thermal conductivity		p	pressure
L	microchannel length			
P	pressure		*Abbreviations*	
q	wall heat flux		CFD	Computational Fluid Dynamics
T	temperature		RCVF	volume fraction of ethanol
U	flow velocity			
ΔP	pressure drop		*Operators*	
			∇	Nabla operator (vector differential operator)
ρ	density			
μ	dynamic viscosity			

1. INTRODUCTION

With the developing trend of high performance, miniaturization, and integration in the electronics industry, the requirement of higher performance of the electronic components becomes demanding. With the decrease of the size of the components, the heat flow density also increases. In general, if the temperature of the electronic products rises 10° sharply, the reliability might be reduced to half of the original value; and when the temperature increases from 75° to 125°, the reliability is reduced

to 20% of the original value. According to the 2007 International Technology Roadmap for Semiconductors, the local power density of integrated circuits has reached 300 W/cm². However, traditional cooling methods have difficulties to meet this cooling requirement. Therefore, several more novel and efficient alternatives have been proposed recently (Schmidt 2003; Kandlikar and Grande 2004a; Saenen and Baelmans 2012; Bermejo *et al.* 2013; Sharma *et al.* 2013; Gong *et al.* 2014). The some of these are:

Saenen and Baelmans (2012) presented a numerical model of a two-phase cooling system using microchannel heat sinks.

Bermejo *et al.* (2013) investigated 20 electronic components in series which need to dissipate a heat flux of 20 kW/m^2 owing to micro evaporators mounted in a refrigeration system. They showed an easy approach to estimate the best design in the space industry.

Sharma *et al.* (2013) modelled a hot water cooled manifold microchannel heat sink for electronic chip cooling. They showed that while increasing viscous dissipation, moderately increased investment of pumping energy can reduce the entropy generation due to heat transfer and thus minimize the overall entropy generation.

Gong *et al.* (2014) numerically investigated the structures of micro-channel heat sinks for chip cooling techniques, four types of heat sinks, including traditional micro-channel heat sink, rectangle column fin heat sink, single-hole jet-cooling heat sink and double-layer micro-channel heat sink. They showed that the layout of microchannel heat sink is very important to the fluid flow and heat transfer. It is positive for improving thermal performance to fill metal foam in the inlet header by strengthening flow distribution uniformity. In comparison to traditional microchannel rows, the pin-fin array way of microchannel arrangement strengthens the thermal performance of the overall heat sink due to the better field coordination characteristic.

Microchannels are fluid flow channels with small hydraulic diameters. Following the classification by Kandlikar and Grande (2004b), channels with a minimum cross-sectional dimension between 200 μm and 3 mm are classified as minichannels and between 1 μm and 200 μm are classified as microchannels. The flow in microchannels has been the subject of increased research interest in the past few years. It is encountered in many important applications, such as miniature heat exchangers, microscale process units, research nuclear reactors, materials processing and thin film deposition technology, biotechnology system as well as in potential space application (Shao *et al.* 2009).

The computational fluid dynamics (CFD) of microchannels has been exploded recently with the improvement computer technique and the suitability of the used models to predict the results (Chao *et al.* 2005; Renksizbulut *et al.* 2006; Hong and Asako 2007; Kuddusi and Cetegen 2009; Shojaeian and Dibaji 2010). The numerical technique in these studies is very important in order to approach the correct result. Qu and Mudawar (2002a; 2002b) used the numerical technique with Simple scheme. Their numerical results showed good agreement with experimental data.

Researches on the effects of the ramification length and angle of the microchannel on pressure drop and heat transfer are very limited in the literature (Li *et al.* 2014), whereas these effects are important for two and multi-phase flows.

In this present work, the effects of the ramification length and angle of the microchannel on pressure drop and heat transfer were investigated because of being an important topic in two and multi-phase, by comparing the computed results with the mathematical model given by Steinke and Kandlikar (2006) and numerical values given in the literature (Chai *et al.* 2011).

The corresponding three-dimensional laminar flow and thermal performance were analyzed numerically by computational fluid dynamics (CFD). A uniform wall heat flux condition was applied on the bottom wall. In order to acquire a better knowledge of the thermal characteristics and mechanisms of the microchannel with T-shaped ramification, the influences of the angle between the two arms of the T profile and T profile length on the pressure drop and heat transfer were discussed in details. Thus, different angles between the two arms of the T-shaped ramification and different lengths of T shaped ramification were designed and studied. However, in order to simplify the paper and illustrate the effect of the angle between the two arms of the T-shaped ramification and the length of T shaped ramification, three typical kinds of the ramification angle with the ramification lengths of 0.25 L and 0.5 L were considered, i.e., 45°, 90°, and 135°. The geometrical dimensions of the microchannel used in the numerical tests had overall length of 10.15 mm and the hydraulic diameter of 133.3 μm. As demonstrated in Fig. 1, the T shaped ramification was located at the center of the straight microchannel with different angles and lengths (for ramification angle 45° and ramification length 0.25 L).
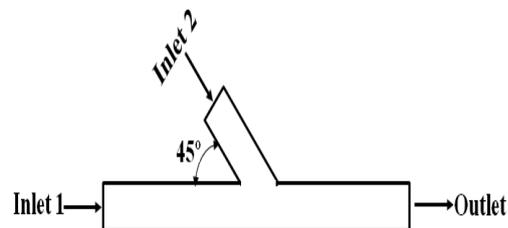
Fig. 1. Shematic demonstration of ramified microchannel for the angle of 45° and the length of 0.25 L.

2. NUMERICAL MODEL

Governing equations for incompressible, steady state and laminar flow in a microchannel were solved numerically using Fluent CFD code.

The steady-state conservation of mass, momentum and energy equations can be written in the following compact form:

$$\nabla . (\rho \vec{U}) = 0 \tag{1}$$

$$\vec{U} . \nabla (\rho \vec{U}) = -\nabla P + \nabla . (\mu \nabla \vec{U}) \tag{2}$$

$$\vec{U} . \nabla (\rho c_p T) = \nabla . (k \nabla T) \tag{3}$$

For the simulations, a uniform heat flux of 670, 1000 and 1500 kW/m² was applied on the bottom surface of the substrate. The top wall surface of the channels and the outer surfaces of the microchannel were assumed to be insulated. For the flow field, the velocity applied at the inlet was assumed to be uniform and a pressure condition was applied at the outlet.

The geometrical dimensions of the microchannel used in the numerical tests had overall length of 10.15 mm and the hydraulic diameter of 133.3 μm.

The numerical computation was performed with a numerical grid shown in Fig. 2.
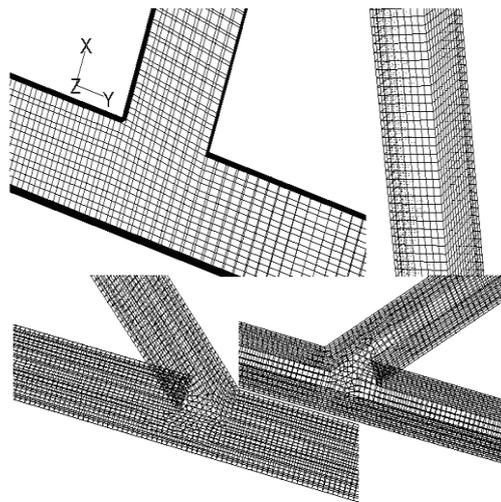
Fig. 2. CFD surface mesh fort the microchannels.

Different grades of grid refinement were tested. The grid refinement study showed that a total number of about 200 000 elements was sufficient to obtain a grid-independent solution.

3. RESULTS AND DISCUSSION

In this paper, to obtain the effect of ramification length and angle of the microchannel on the pressure drop and heat transfer, the 3-D numerical simulations of the microchannels for different geometric parameters were evaluated. The angle between the two arms of the T profile and the ramification length were varied and different inlet velocities were considered. The corresponding ranges of the pumping power and Reynolds number were examined in detail.

Comparison of pressure drop values obtained by numerical tests with mathematical model by Steinke and Kandlikar (2006) is given Fig. 3.

As can be seen from Fig. 3, the pressure drop increases with the increasing inlet velocity, so it is clear that the consumption of pumping power directly increases. Results obtained from the numerical tests show good agreement with the mathematical model and the maximum deviation is less than 2.12%.
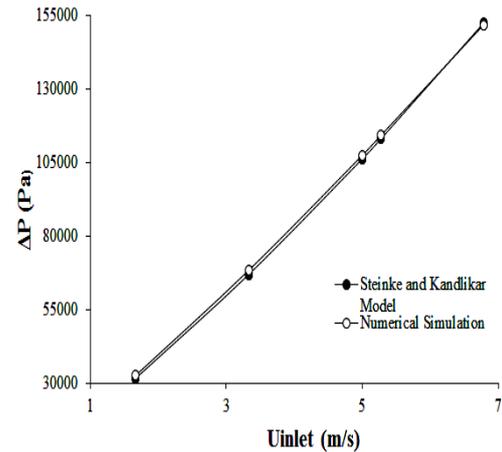
Fig. 3. Comparison of the pressure drops among the computed results and the mathematical model.

Fig. 4 gives the temperature contour obtained by solving the energy equation, for the inlet velocity of 3.45 m/s and at x=0.25 mm.
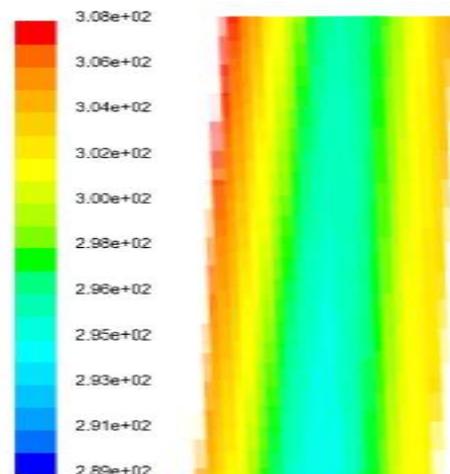
Fig. 4. Temperature contour obtained for the inlet velocity of 3.45 m/s and at x=0.25 mm.

The inlet temperature of fluid had a constant value of 289 K. A uniform heat flux, q=0.67 MW/m²), was applied to the bottom surface of the microchannel. The maximum value of the temperature given in ref. Chai *et al.* (2011) was about 308 K.

After these validation studies, ramified microchannel was modeled and the effects of the ramification length and angle on the pressure drop and the heat transfer were investigated in detail.

Fig. 5 shows a comparison of the pressure drops for two ramification lengths of microchannel at different inlet velocities. As can be seen from Fig. 5, the maximum difference between the pressure drops for two lengths is 3.45%. However, the increase in temperature has a negligible level (Fig. 6).
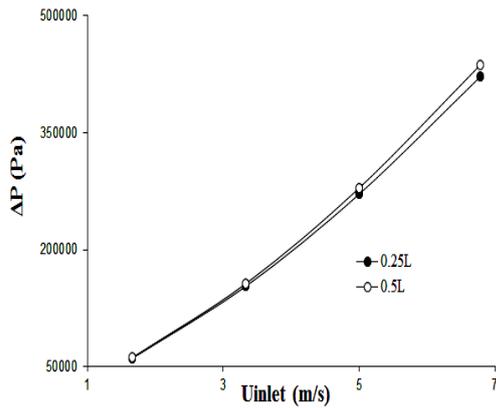
Fig. 5. Pressure drops for two ramification lengths of microchannel at different inlet velocities.
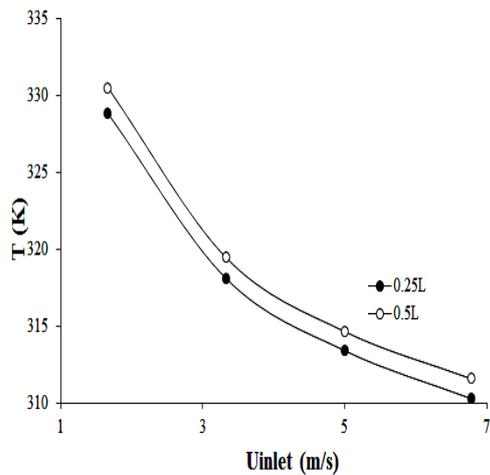
Fig. 6. Temperatures for different ramification lengths and different inlet velocities at a uniform heat flux from the bottom of microchannel, q=0.67 MW/m².

Fig. 6 shows the relationship between the maximum temperatures of a ramified microchannel for a range of inlet velocities. It can be seen that the maximum temperature decreases with the increasing inlet velocity because the thermal resistance decreases as the inlet velocity increases. This nonlinear trend is in agreement with already published work in literature (Bello *et al.* 2010). As the length of the T profile becomes bigger, the pressure drop becomes higher at the same inlet velocities. Thus the pressure drop of ramification length of 0.25L is smaller than that of the other case. However, the smallest pressure drop is found for smooth microchannel compared with ramified microchannel (Fig. 7). In other words, the T-shaped ramification not only improves the thermal performance of the microchannels, but also increases the pressure drop.

Fig. 8 shows a comparison of the pressure drops for 0.25L according to the ramification angle measured from the microchannel axis. As can be seen from this figure, the increase in the ramification angle appears to increase the pressure drop. The reason is that the fluid flow disrupts with the increase in the ramification angle. These results demonstrate that

the ramification angle in a ramified microchannel should be a small angle.
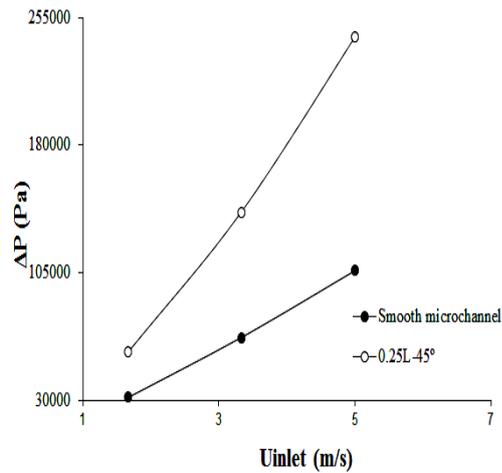
Fig. 7. Pressure drops among the smooth microchannel and the ramified microchannel with 0.25L-45°.
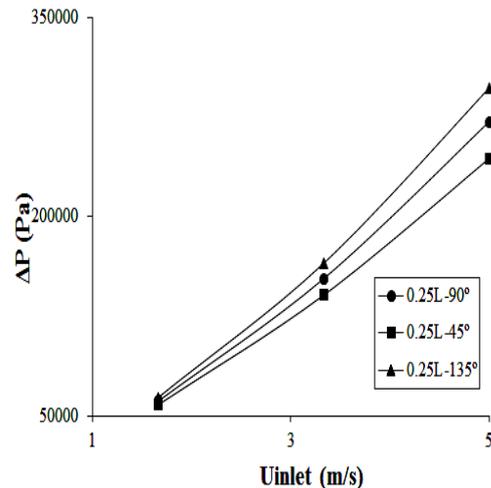
Fig. 8. Pressure drops for 0.25L according to the ramification angle as from the microchannel inlet axis.

Fig. 9 shows a comparison of the heat transfer coefficients for 0.25L with a constant fluid inlet temperature, 289 K, and a constant inlet velocity, 5 m/s, and different uniform heat fluxes from the bottom surface of microchannel, q=670, 1000 and 1500 kW/m².

Fig. 9 shows the effects of heat fluxes on the heat transfer coefficient. It is obvious that the heat flux affects the heat transfer coefficient. At First, the heat transfer coefficient increases with increasing the heat flux, and then it almost becomes constant due to transition of flow to the fully developed flow. The reason is that the fluid flow in the microchannel appears a transition from partial to fully developed boiling.

Fig. 10 gives a comparison of the pressure drops with a constant uniform heat fluxes from the bottom surface of microchannel, q=670 kW/m² by changing the ratio of the volume fraction at the inlet of the

770

microchannel in 0.25 L length. The RCVF shorting in this figure means the volume fraction of ethanol in the ramification inlet. As for the fluid in the main microchannel, it is only water. As can be seen from this figure, the increase in the ratio volume fraction of ethanol appears to decrease the pressure drop. These results demonstrate that the properties of fluid pattern significantly affect pressure drop.
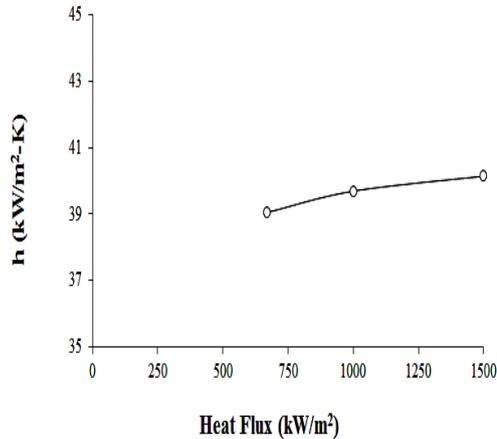
Fig. 9. Heat transfer coefficients for 0.25L with a constant fluid inlet temperature, 289 K, and a constant inlet velocity, 5 m/s, and at different heat fluxes.
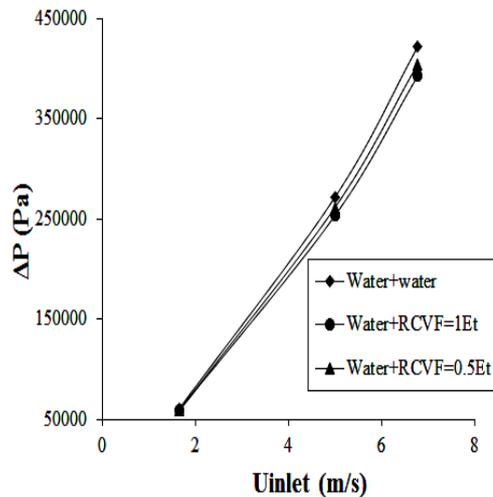
Fig. 10. Pressure drops obtained by changing volume fraction ratio at different inlet velocities.

Fig. 11 shows a comparison of the maximum temperatures inside the ramified microchannel obtained by changing volume fraction from the ramification inlet with a constant water flow in the main microchannel for 0.25L with a constant fluid inlet temperature, 289 K, and a constant inlet velocity, 5 m/s, and different uniform heat fluxes from the bottom surface of microchannel, q=670, 1000 and 1500 kW/m^2. As can be seen from Fig. 11, the increase in the ratio volume fraction of ethanol appears to increase the maximum temperature inside the ramified microchannel. These results demonstrate that the properties of fluid pair significantly affect heat transfer. And, it

can be concluded that the improvement of the heat transfer in the ramified microchannel relates to the properties of fluid pattern.
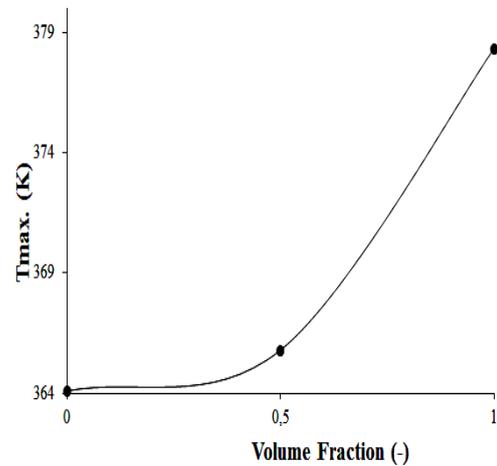
Fig. 11. Maximum temperatures obtained by changing volume fraction ratio for U$_{inlet}$=1.667 m/s.

4. CONCLUSION

In this study, the effects of the ramification length and angle of the microchannel on the pressure drop and the heat transfer were investigated because of being an important topic in two and multi-phase flows, by comparing the computed results with the mathematical model given by Steinke and Kandlikar (2006) and numerical values in the literature (Chai *et al*. 2011).

The pressure drop increases with the increasing the ramification length because of increasing friction area.

The maximum temperature increases slightly with the increasing the ramification length because of distribution area. However, this increase has a negligible level.

The increase in the ramification angle measured from the microchannel axis appears to increase the pressure drop. The reason is that the fluid flow disrupts with the increase in the ramification angle. These results demonstrate that the ramification angle in a ramified microchannel should be a small angle.

The heat flux affects considerably on the heat transfer coefficient. At first the heat transfer coefficient increases with increasing the heat flux, and then it almost becomes constant due to transition of flow to the fully developed flow. The reason is that the fluid flow in the microchannel appears a transition from partial to fully developed boiling.

The increase in the ratio volume fraction of ethanol appears to increase the maximum temperature inside the ramified microchannel. These results demonstrate that the properties of fluid pair significantly affect heat transfer. And, it can be concluded that the improvement of the heat transfer

in the ramified microchannel relates to the properties of fluid pattern.

REFERENCES

Bello, O.T., J. P. Meyer and F. U. Ighalo (2010). Combined numerical optimization and constructal theory for the design of microchannel heat sinks. *Num. Heat Trans; Part A 58*, 882-899.

Bermejo, P., R. Revellin, R. Charnay, O. Garbrecht, J. Hugon and J. Bonjour (2013). Modeling of a microchannel evaporator for space electronics cooling:entropy generation minimization approach. *Heat Trans. Eng. 34(4)*, 303-312.

Cao, B., G. W. Chen and Q. Yuan (2005). Fully developed laminar flow and heat transfer in smooth trapezoidal microchannel. *Int. Comm. in Heat and Mass Trans. 32*, 1211–1220.

Chai, L., G. Xia, M. Zhou and J. Li (2011). Numerical simulation of fluid flow and heat transfer in a microchannel heat sink with offset fan-shaped reentrant cavities in sidewall. *Int. comm. in Heat and Mass Trans. 38*, 577–584.

Gong, L., J. Zhao and S. Huang (2014). Numerical study on layout of micro-channel heat sink for thermal management of electronic devices. *App. Therm.Eng.* 2014.09.048.

Hong, C. and Y. Asako (2007). Heat transfer characteristics of gaseous flows in a microchannel and a microtube with constant wall temperature. *Num. Heat Trans. Part A 52*, 219–238.

Kandlikar, S. G. and W. J. Grande (2004a). Evolution of single phase flow in microchannels for high heat flux chip cooling-thermalhydraulic performance enchancement and fabrication technology. *Heat Transfer Eng. 25*, 5–16.

Kandlikar, S. G. and W. J. Grande (2004b). Evolution of microchannel flow passages–thermohydraulic performance and fabrication technology. *Heat Transfer Eng. 24*, 3–17.

Kuddusi, L. and E. Cetegen (2009). Thermal and hydrodynamic analysis of gaseous flow in trapezoidal silicon microchannels. *Int. J. of Thermal Sci. 48*, 353–362.

Li, Y., F. Zhang, B. Sunden and G. Xie (2014). Laminar thermal performance of microchannel heat sinks with constructal vertical Y-shaped bifurcation plates. *Applied Therm. Eng. 73*, 183-193.

Qu, W.L. and I. Mudawar (2002a). Experimental and numerical study of pressure drop and heat transfer in a single-phase microchannel heat sink. *Int. J. of Heat and Mass Trans. 45*, 2549-2565.

Qu, W.L. and I. Mudawar (2002b). Analysis of three-dimensional heat transfer in microchannel heat sink. *Int. J. of Heat and Mass Trans. 45*, 3973-3985.

Renksizbulut, M., H. Niazmand and G. Tercan (2006). Slip-flow and heat transfer in rectangular microchannels with constant wall temperature. *Int. J. of Thermal Sci. 45*, 870–881.

Saenen, T. and M. Baelmans (2012). Numerical model of a two-phase microchannel heat sink electronics cooling system. *Int. J. of Thermal Sci. 59*, 214–223.

Schmidt, R. (2003). Challenges in electronic cooling: opportunities for enhanced thermal management techniques-microprocessor liquid cooled minichannel heat sink. *First Int. Conf. on Microchannel and Minichannel, Rochester 1*, 951-959.

Shao, N., A. Gavriilidis and P. Angeli (2009). Flow regimes for adiabatic gas–liquid flow in microchannels. *Chem. Eng. Sci. 64*, 2749-2761.

Sharma, C. S., M. K. Tiwari, B. Michel and D. Poulikakos (2013). Thermofluidics and energetics of a manifold microchannel heat sink for electronics with recovered hot water as working fluid. *Int. J. of Heat and Mass Trans. 58*, 135-151.

Shojaeian, M. and S. A. R. Dibaji (2010). Three-dimensional numerical simulation of the slip flow through triangular microchannels. *Int. Comm. in Heat and Mass Trans. 37*, 324-329.

Steinke, M. E. and S. G. Kandlikar (2006). Single-phase liquid friction factors in microchannel. *Int. J. of Thermal Sci. 45*, 1073-1083.